

We are IntechOpen, the world's leading publisher of Open Access books Built by scientists, for scientists

6,900

Open access books available

185,000

International authors and editors

200M

Downloads

Our authors are among the

154

Countries delivered to

TOP 1%

most cited scientists

12.2%

Contributors from top 500 universities



WEB OF SCIENCE™

Selection of our books indexed in the Book Citation Index
in Web of Science™ Core Collection (BKCI)

Interested in publishing with us?
Contact book.department@intechopen.com

Numbers displayed above are based on latest data collected.
For more information visit www.intechopen.com



In-Office Dispersion and Exposure to Contaminants Originating from an Unfolded Letter

Alfred D. Eisner¹, Russell W. Wiener² and Jacky Rosati²

¹*Alion Science and Technology,*

²*National Homeland Security Research Center,*

U.S. Environmental Protection Agency,

USA

1. Introduction

Incidents of bioterrorism that have occurred over the past decade have demonstrated a need to understand the transmission and exposure risks of daily activities to potential biological agents (NATO, 2005; de Armond, 2002; Block, 2001). Based on experience since September 11, 2001, the mail has become a significant means of bioagent dispersion. This chapter seeks to further advance our understanding of fluid and aerosol dynamic processes of exposures resulting from dust lying on the surface of a letter or a table being resuspended by air flow, (Richmond-Bryant, et al., 2006).

Transmission of aerosols from an unfolded letter, (Duncan et al., 2009), is dependent on the motion of the air in the environment in which the letter resides (Dull et al., 2002). The primary source of fluid motion in most buildings is the heating, ventilation, and air-conditioning (HVAC) system. Several reports suggest that numerous pathogens may survive such airborne transport (e.g., Nardell et al., 1986; Mangili and Gendreau, 2005). Others show how contaminants can be dispersed into the indoor environment (e.g., reviews by Wallace, 1996, and Nazaroff, 2004; Price, et al., 2009; Reshetin & Regens, 2003; Reshetin & Regens, 2004). These reviews and many papers cited therein show that indoor particle transport is subject to complex interactions of dispersion, deposition, and resuspension. Understanding these processes is predicated on understanding the interaction between turbulent airflow and particles. Rooms often have complex geometries that result in extremely complex turbulence because of flow phenomena such as flow separation, recirculation, and buoyancy (Posner et al., 2003; Rim and Novoselac, 2009).

Contamination and exposure resulting from a localized source such as a contaminated letter has received some recent attention. (Agranovski et al., 2005; Ho et al., 1993; Ho et al., 2005; Kornikakis et al., 2001; Kornikakis et al., 2009; Kornikakis et al., 2010; Lien et al., 2010).

In many offices, outlets from the HVAC system are positioned in the ceiling and often generate a substantial downward blowing of air, (Nardell, et al., 1986). Ceiling fans can have a similar effect. This airflow will almost certainly incorporate flow separation and recirculation zones. Advancing the understanding of dispersion of particulate contaminants under such complex conditions can provide useful input for decontamination efforts

directed toward contaminated individuals or objects. To this end, the study described in this paper investigated dispersion and surface contamination resulting from contaminated material being reentrained from flat letter lying on a table top under a vent.

2. Methods

2.1 Experimental setting

This investigation was designed to explore a hypothetical situation in which a person seated at a table is exposed to reentrained dust from the surface of a letter that is lying flat on a desk under an HVAC vent. In our experimental simulation, an individual, represented by a manikin, was seated at a table adjacent to an office wall and positioned under an HVAC vent (Fig. 1). A surrogate letter was made of Rosco cine foil™, matte black, and gauge 0.002 in. Its thickness, stiffness and roughness were similar to a standard paper sheet. Using this surrogate was necessary to prevent PIV cameras over saturation and to obtain images of particles moving very close to the surface. From now on we will refer to this surrogate letter as letter. It was placed flatly on the table in front of the manikin and sprinkled with test dust. The dust was Arizona dust with particle size ranging from 1-5 microns.

2.2 Experimental systems

Several fundamental experimental systems were used in this research: a thermal articulated manikin (TAM), an environmental walk-in chamber (EWC) used as an office space simulator, and a particle imaging velocimetry (PIV) system. Each of these systems is described briefly below.

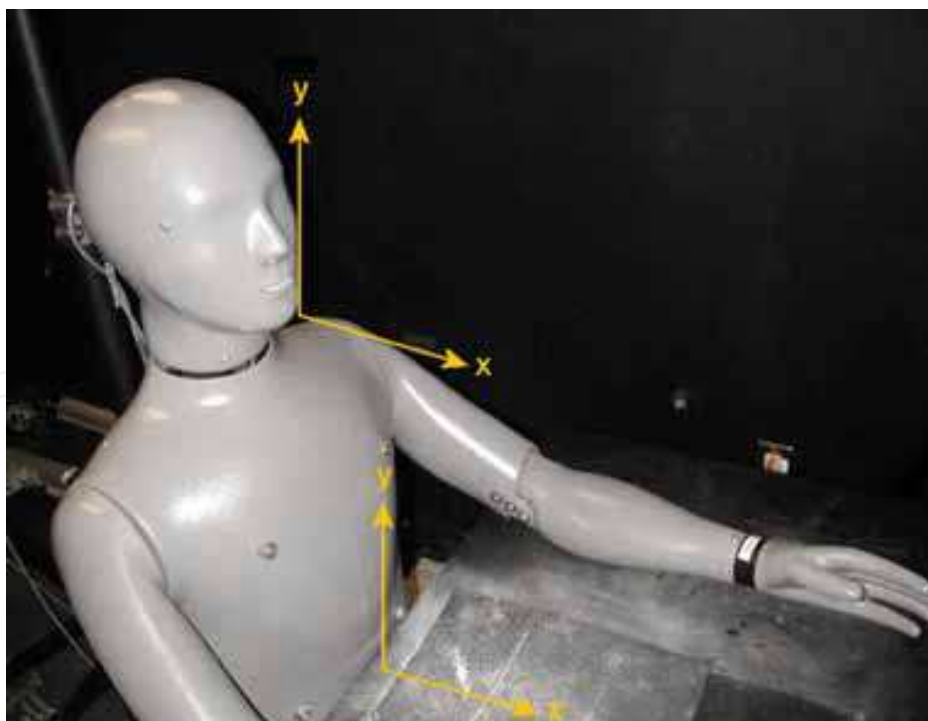


Fig. 1. Manikin confronted by a cloud of contaminating dust blown from an unfolded letter by air from a ceiling vent. Piled-up dust of mostly agglomerated and shifted large particles can be seen on the letter section close to the manikin's chest. Two x,y coordinate systems reflect positions of the PIV test areas, namely, a table area and a head area.

2.2.1 Articulated manikin

An adult-size TAM (Model Newton, Measurement Technology Northwest, Seattle, WA, USA) with 18 heating zones was used in this study. The dimensions of the manikin were sized to match a 50th percentile U.S./European male. The TAM, designed as a repeatable instrument to evaluate various thermal conditions, has isothermal surfaces over each individual zone. All thermal zones are fitted with heaters to simulate metabolic heat output rates and a distributed temperature sensor to accurately measure the average temperature over each zone. For the purpose of this study all zones were set at 37 °C.

2.2.2 Environmental walk-in chamber

The EWC (297 by 216 by 221 cm) was made of industrial steel and was located inside a large laboratory facility with temperature and humidity kept at normal laboratory levels. The EWC was fitted with two ceiling openings (20 cm in diameter) located centrally 50 cm from the front and back walls. The openings were used as the HVAC system's air inlet and outlet and were connected to the recirculating air moving unit positioned on the roof of the EWC. The air mover speed could be controlled by a variac, and the blower fan could be turned on or off as needed. Aluminum corrugated duct work several meters long was connected to the blower to allow for quick heat dissipation by the blower fan, thus ensuring the temperature and humidity conditions inside the EWC were essentially those in the large laboratory space. A table measuring 122 by 70 by 91 cm and a TAM were positioned inside the EWC.

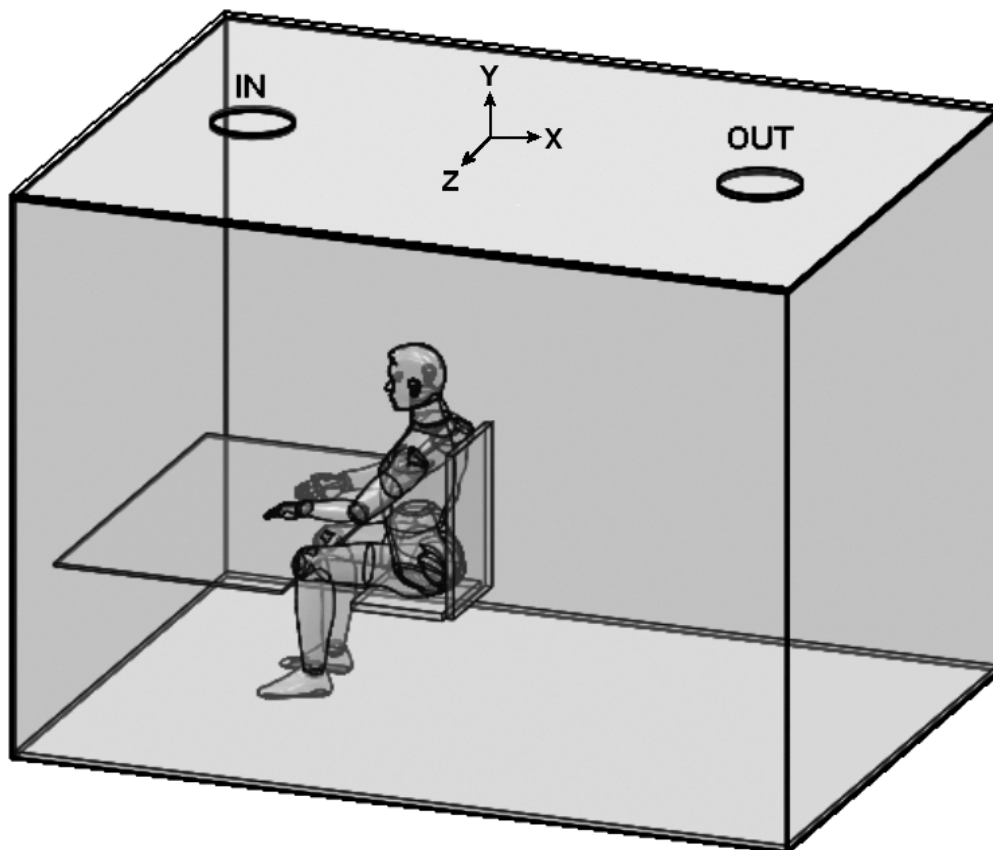


Fig. 2. Schematic view of TAM seated inside EWC. The table and chair are represented schematically by flat rectangles. Two openings in the ceiling represent the HVAC inlet (IN) (above the table) and outlet (OUT).

2.2.3 Particle imaging velocimetry (PIV)

A two-pulse laser technique such as PIV (TSI Inc., Shoreview, MN, USA) is commonly used to investigate particle-laden fluid flows. In these laboratory configurations, two laser pulses are fired in rapid sequence, typically 10 microseconds to 10 milliseconds apart. Usually two synchronized laser heads are used. In this study, a standard PIV configuration was used in which two laser beams following a common path form sheets that illuminate a plane of air, thus illuminating the location of particles in the flow. Two PIV digital cameras capable of recording two frames in one image were used. PIV was activated remotely to collect images of the dispersed dust particles. The images were then analyzed for particle displacement, allowing study of the flow. The images were analyzed using Insight 3G software provided by the PIV manufacturer (TSI, Inc.). This application can execute statistical analysis and generate 2-D and 3-D graphics in conjunction with applications such as TechPlot (Polysoft, Salt Lake City, UT, USA) and Matlab (The MathWorks, Inc., Natick, MA, USA).

2.3 Numerical methods

Computational fluid dynamics (CFD) numerical methods, (Darrell, et al., 2007), were used to simulate and analyze airflow patterns and thermal fields inside the chamber and around the manikin (Lu et al., 1997; Patankar, 1980). The CFD method is predicated on solving the Navier-Stokes equations, which are formulations of mass, momentum, and energy conservation laws for fluid flows. The equations are supplemented by fluid state equations defining the nature of the fluid and by empirical dependencies of fluid density, viscosity, and thermal conductivity on temperature.

To predict turbulent flow, the Favre-averaged Navier-Stokes equations were used, where time-averaged effects of the flow turbulence on the flow parameters were considered. In this procedure, the information on Reynolds stresses must be provided for the equations. To close this system of equations, transport equations for the turbulent kinetic energy and its dissipation rate, the so-called k - ϵ model, are employed. A laminar/turbulent boundary layer model was used to describe flows in near-wall regions. The model was based on the modified wall functions approach. This model is employed to characterize laminar and turbulent flows near the walls and to describe transitions from laminar to turbulent flow and vice versa. The modified wall function uses a Van Driest's profile instead of a logarithmic profile. If the size of the mesh cell near the wall is more than the boundary layer thickness, the integral boundary layer technology is used.

The CFD model calculates two-phase flows as a motion of spherical solid particles in a steady-state flow field. Their drag coefficient is calculated with Henderson's formula, derived for continuum laminar, transient, and turbulent flows over the particles and taking into account the temperature difference between the fluid and the particle. The gravity is also taken into account. The interaction of particles with the model surfaces is taken into account by specifying ideal or non-ideal reflection (which is typical for solid particles). The ideal reflection denotes that, in the impinging plane defined by the particle velocity vector and the surface normal at the impingement point, the particle velocity component tangent to the surface is conserved, whereas the particle velocity component normal to the surface changes its sign. A non-ideal reflection is specified by the two particle velocity restitution (reflection) coefficients.

Briefly, the CFD program solves the governing equations with the finite volume (FV) method on a spatially rectangular computational mesh designed in the Cartesian coordinate

system with the planes orthogonal to its axes and refined locally at the solid/fluid interface and, if necessary in specified fluid regions, at the solid/solid surfaces and in the fluid region during calculation. Values of all the physical variables are stored at the mesh cell centers. In the FV method, the governing equations are discretized in a conservative form. The spatial derivatives are approximated with implicit difference operators of second-order accuracy. The time derivatives are approximated with an implicit first-order Euler scheme. The viscosity of the numerical scheme is negligible with respect to the fluid viscosity. All issues related to solution convergence, such as meshing or boundary flow convergence, are taken care of automatically or by user defined criteria.

A numerical (virtual) EWC (NEWC), as shown in Fig. 2, was used to model the airflow and aerosol dispersion inside the simulated office, (Rhie & Chow, 1983; Vlahostergios, et al., 2009). The dimensions of the NEWC were identical to the actual EWC. The NEWC is a fully functional meshed 3-D numerical model of the EWC and the articulated manikin seated at the table. The manikin's position and orientation could be changed and the chamber furnishings rearranged as desired. The NEWC was fitted with two ceiling vents that could be used to define air in-flow and out-flow as desired based on volume or pressure. For simulations, the wall temperature and the manikin's body temperature were 20 °C and 37 °C, respectively, based on actual experimental conditions.

2.4 Experiments

2.4.1 Table zone tests

In our experiments, the letter was folded as a trifold letter and then unfolded and placed on the desk. It was positioned at two locations in the EWC: (1) close to the vent with the center of the letter at 30 cm from the manikin's chest and (2) close to the manikin's chest with the center of the page at 20 cm from the manikin's chest. The letter was coated (contaminated) with dust. The dust coating was achieved by loading a small amount of fine test dust (Powder Technology, Inc., Burnsville, MN, USA) in the 5 µm or less size range onto a No. 270 sieve and vigorously shaking the sieve above the foil. Experiments were conducted with the EWC closed and no laboratory personnel present to reduce any uncontrolled disturbance to air motion.

The vertical test area measured 25 by 25 cm and was located directly above the letter in the vertical plane bisecting the manikin's chest, as indicated by the x,y coordinate system shown just above the table in front of the manikin's chest in Fig. 1. The coordinate system origin was located on the table surface 5 cm from the manikin's chest. Thus, the x-axis coincided with the table surface and extended from the manikin toward the wall of the test room, while the y-axis extended vertically upwards. (Note that because of various limitations, such as accessibility inside the EWC, PIV camera positioning and viewing orientation, and a separate CFD-defined calculational domain, several coordinate systems appear in images and figures in this paper.)

The HVAC system was activated simultaneously with the PIV system to capture the event of the dust being reentrained from the foil. The PIV system could collect 20 double images in real time (saved in ROM) at a frequency of up to 10 images per second. Thus, to increase the possibility of detecting particle liftoff from the letter, we kept the PIV frequency at 2-3 images per second. These experiments showed that dust particles were indeed blown from the letter and reached the breathing zone of the manikin, as discussed below.

2.4.2 Breathing zone tests

After demonstrating in the table zone tests that particles could be lifted from the contaminated letter, experiments were conducted to determine if these particles reached the manikin's breathing zone. For the purpose of these experiments, the PIV test section was positioned in front of the manikin's head. This positioning is reflected by the x,y coordinate system adjacent to the manikin's face (see Fig. 1). Experimental procedures were similar to those in the previous experiments.

3. Experimental results and analyses

3.1 Airflow pattern in table zone area

Several experiments were conducted with theatrical smoke particles fed into the air duct system to determine the airflow pattern above the table. When the blower was activated, the air velocity from the vent quickly reached approximately 1 m s^{-1} . PIV images of the entire test area were then analyzed. Representative velocity vector fields, measured within a second of each other, are shown in Fig. 3a and 3b.

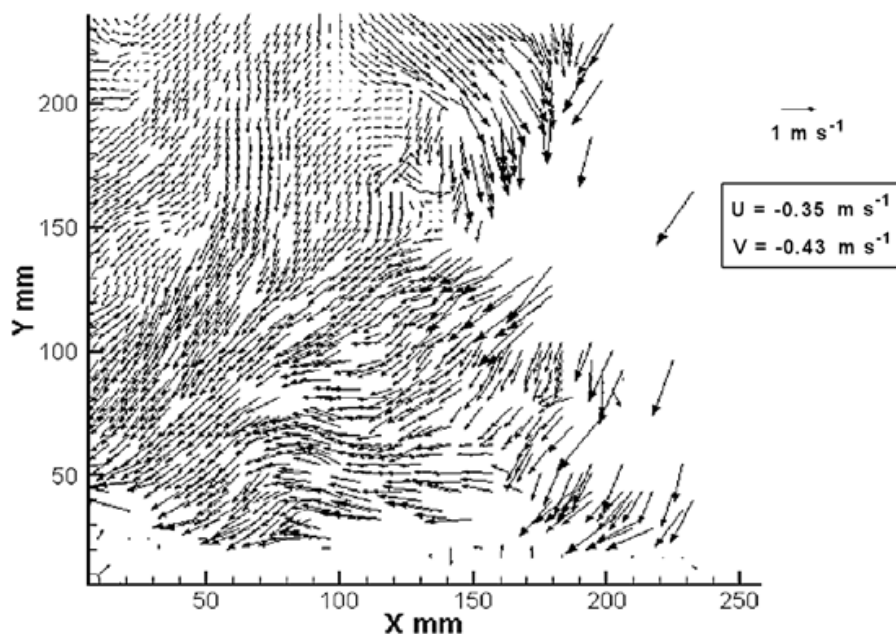


Fig. 3a. Airflow vector field in PIV test area just above the letter. Manikin's torso is to the left of the y-axis. For the investigation area shown, the average U (horizontal) velocity component was -0.35 m s^{-1} , and the average V (vertical) velocity component was -0.43 m s^{-1} .

Areas void of vectors, especially in Fig. 3a, most likely resulted from the lack of particles at the instant the image was taken. The smoke generator was delivering particles directly into the venting duct and images were captured before well-mixed conditions were achieved.

A comparison of Fig. 3a and 3b shows that the velocities in Fig. 3b are generally higher than in Fig. 3a, because these images were captured as the blower was speeding up. The higher velocity resulted from activation of the air mover and its rapid acceleration to the steady maximum rate. Part of the airflow is diverted by the table toward the manikin's chest, especially within the layer 10 cm from the table surface. Although the average velocity components during those seconds when the images were captured were on the order of 0.5 m s^{-1} , the increased vector lengths in Fig. 3a and 3b show that the velocity of the air flowing parallel to the table surface in that layer was higher and exceeded 1 m s^{-1} .

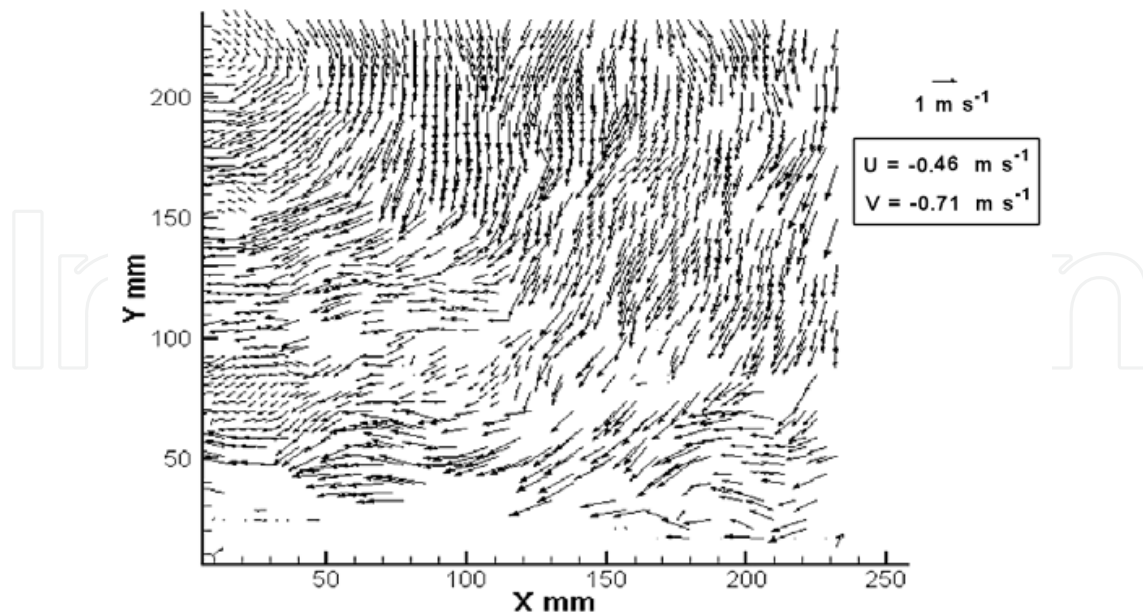


Fig. 3b. Airflow vector field in PIV test area just above the letter. The manikin's torso is to the left of the y-axis. For the investigation area shown, the average U (horizontal) velocity component was -0.46 m s^{-1} , and the average V (vertical) velocity component was -0.71 m s^{-1} .

3.2 Contaminated letter tests

In these experiments, the air mover and the PIV system were activated simultaneously to capture images of the dust being blown from the letter. Particle motion away from the edge of the letter is visible in Fig. 4a in the form of a particle cloud. This area was analyzed to produce the particle velocity vector field shown in Fig. 4b. Although particle motion toward the manikin's chest was a dominating characteristic of the transport, some particle motion was affected by the flow separation from the letter edge.

Suspecting that higher average horizontal air velocities may exist along the table surface farther from the vent's central axis stagnation area, the letter was positioned closer to the manikin, at 20 cm from the chest. The event is shown in Fig. 5a and its corresponding velocity field in Fig. 5b.

As expected, this experiment resulted in higher average horizontal particle velocities than in the previous case. Positioning the letter somewhat farther away from the vent resulted in particles being subjected to a less chaotic and more developed boundary airflow pattern. Such velocities can certainly be effective in delivering the dust to the manikin's chest.

Although these data produced clear, quantifiable evidence that particles on the contaminated foil can become airborne, some particles became deposited on the table surface, thus contaminating the table surface as shown in Fig. 6. The initial powder coating of the letter was very fine. The air jet affected the particles in a unique way: namely, particles traversed the surface and in the process agglomerated into much larger particles that are easily visible on the page surface and the table surface. Many particles followed that airflow below the table edge and contaminated lower parts of the manikin's torso in the process.

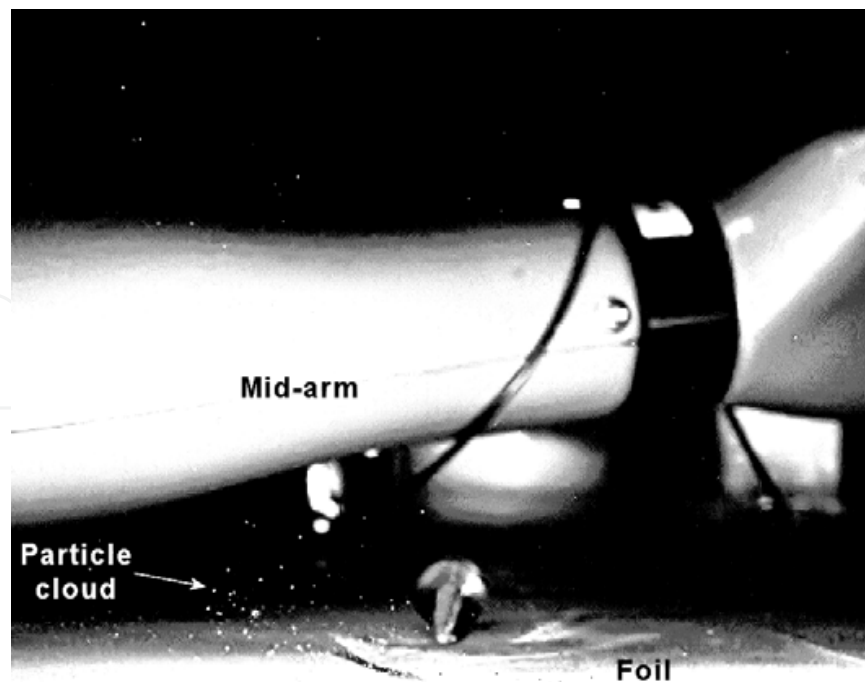


Fig. 4a. Cloud of particles (under mid-arm) moving away from the letter positioned 30 cm from the chest by air emerging from the ceiling vent.

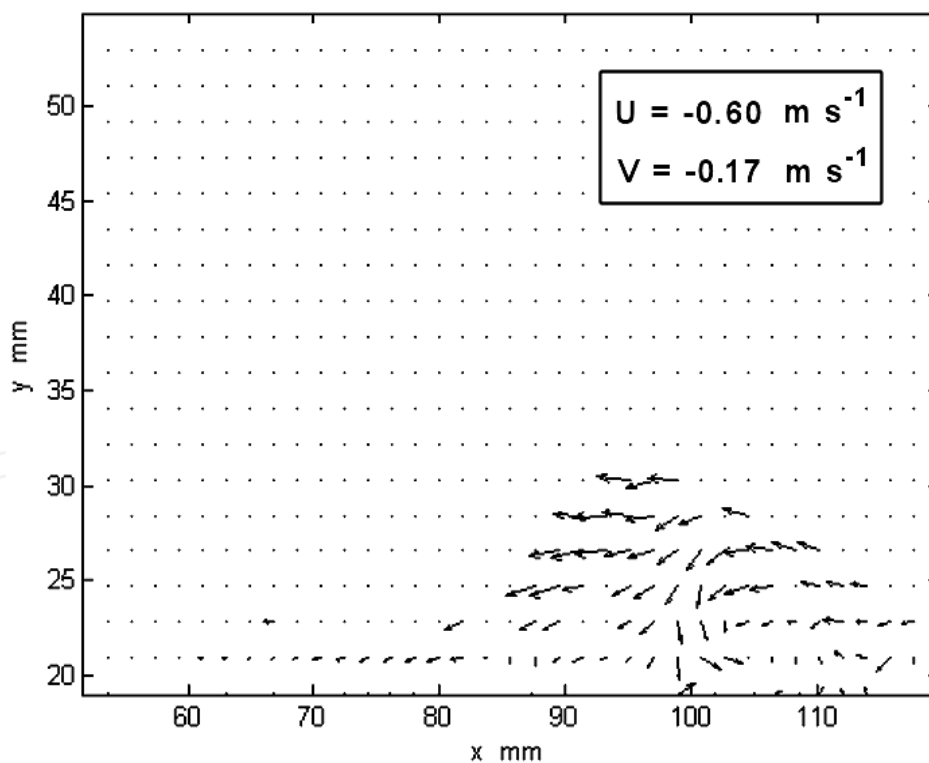


Fig. 4b. Air velocity field obtained using particles lifted from the letter positioned 30 cm from the chest. The average U (horizontal) velocity component was -0.60 m s^{-1} , and the average V (vertical) velocity component was -0.17 m s^{-1} . The letter surface is essentially at $y = 20 \text{ mm}$. (Values smaller than $y = 20 \text{ mm}$ pertained to the part of the image irrelevant to particle transport.)

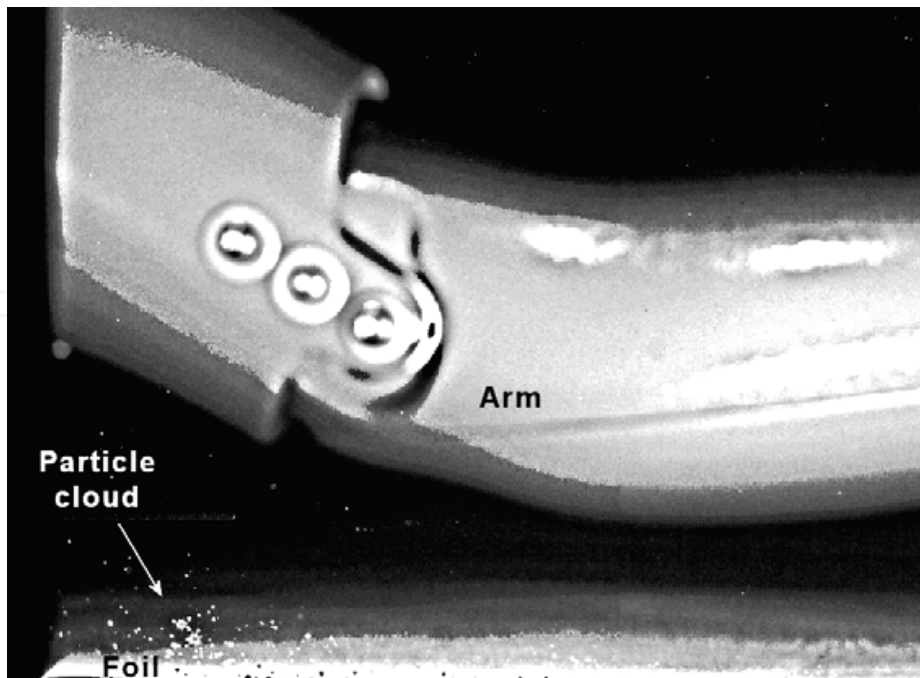


Fig. 5a. Contaminant particles (lower left corner of image) being moved from letter positioned 20 cm from the chest by air emerging from the vent.

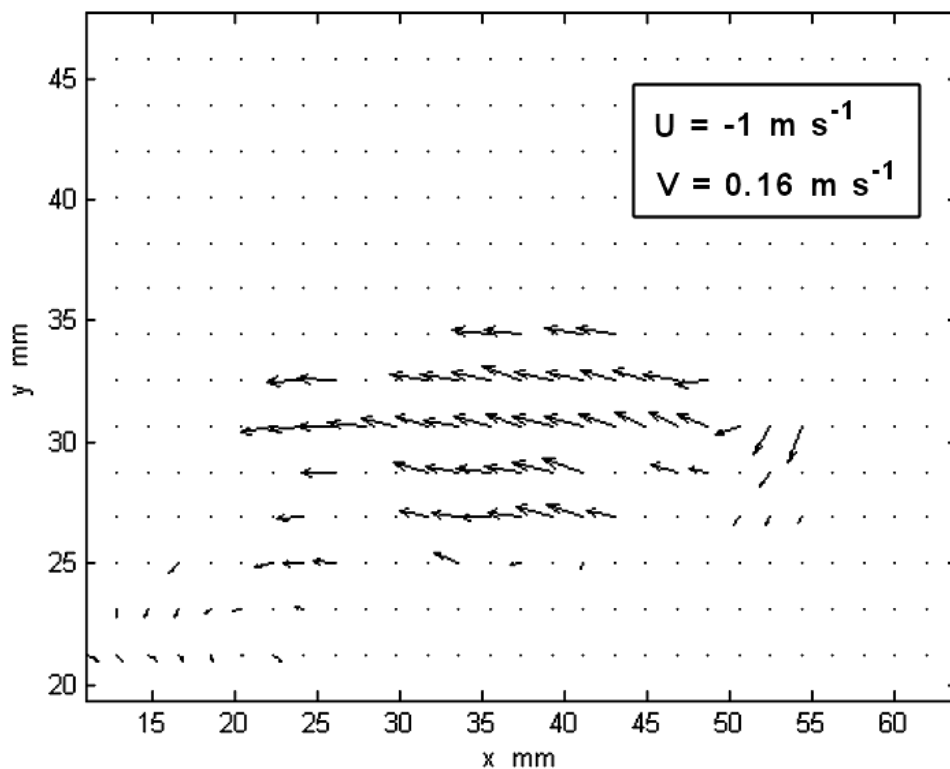


Fig. 5b. Velocity field within 10 mm of the letter surface obtained using particles lifted from the letter. The average U (horizontal) velocity component was approximately -1 m s^{-1} , and the average V (vertical) velocity component was 0.16 m s^{-1} . The letter surface is essentially at $y = 25 \text{ mm}$. (Values smaller than $y = 25 \text{ mm}$ pertained to the part of the image irrelevant to particle transport.)

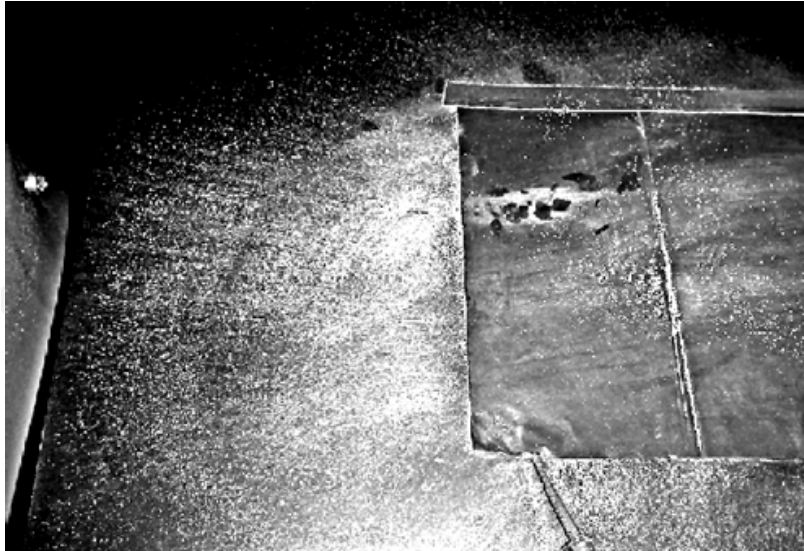


Fig. 6. Dust pattern created by air from the vent as dust is blown from the letter. The manikin is positioned to the left from the table edge visible in this figure.

3.3 Breathing zone tests

To determine whether particles reentrained from the letter reached the manikin's breathing zone, PIV images were analyzed to obtain a velocity vector field like the one in Fig. 7. A few seconds later a residual smoke aerosol entered the airflow and allowed detailed observation of the airflow in front of the manikin's face. The flow pattern is shown in Fig. 8. Strong deflection by the chin and other facial features is noticeable. In addition, the orientation of the flow vectors also suggests the possibility that a recirculation zone is created in front of

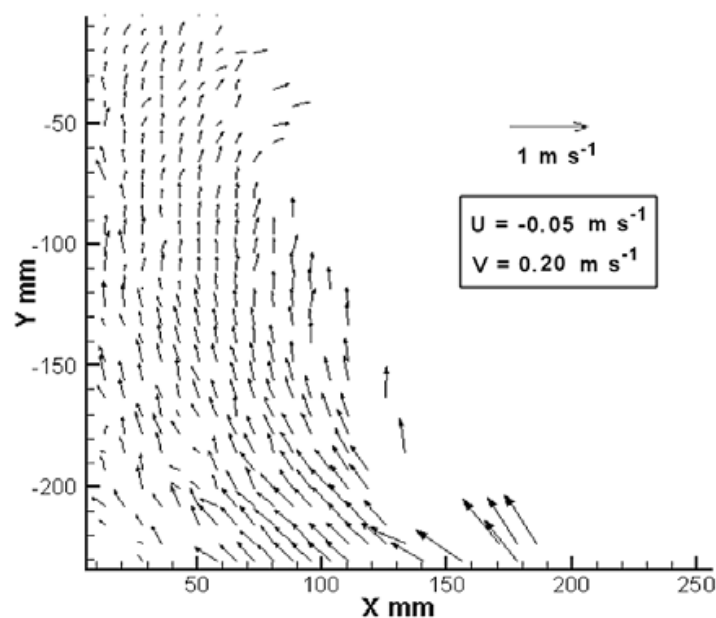


Fig. 7. Airflow vector field in the PIV test area in front of the face, created entirely by particles lifted from the contaminated letter. The manikin's head is positioned to the left of the y-axis. The average U (horizontal) velocity component was -0.05 m s^{-1} , and the average V (vertical) velocity component was 0.2 m s^{-1} . $Y = 0$ corresponds to the top of the manikin's head, a convenient point of reference. $X = 0$ is adjacent to the manikin's face.

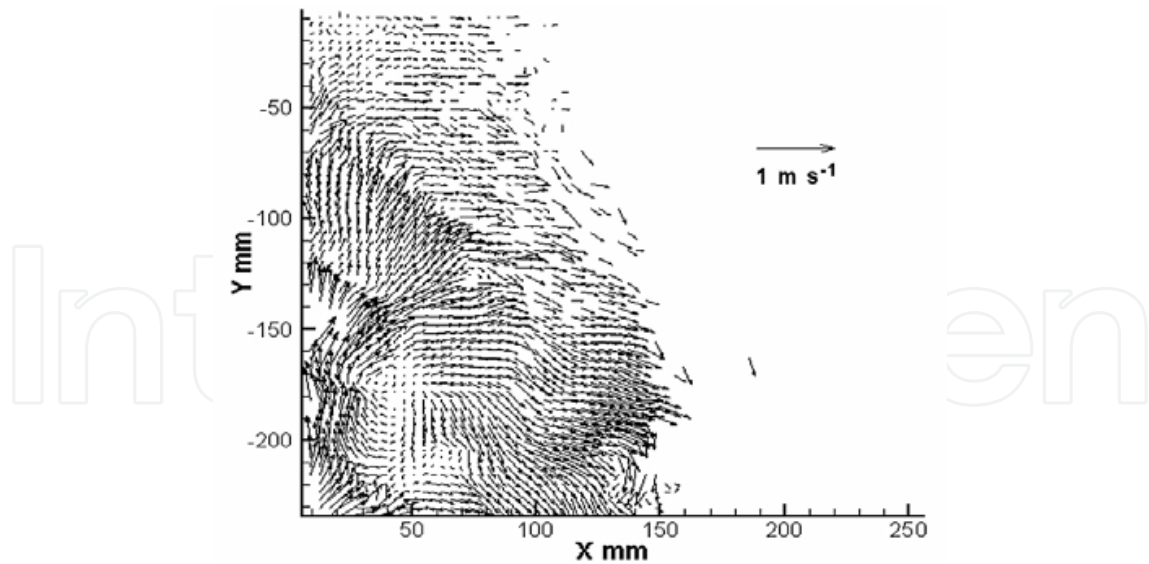


Fig. 8. Detailed airflow pattern in front of the manikin's face, as depicted by the smoke particles carried by the vent air. $Y = 0$ corresponds to the top of the manikin's head, a convenient point of reference. $X = 0$ is adjacent to the manikin's face

and slightly below the head zone. Such recirculation can lead to a longer exposure time. The very few vectors after approximately $x = 130$ is likely due to lack of light sheet in that area. Here the light sheet (shaped triangularly) originated from above the manikin's head to illuminate the area as close to the face as possible.

4. Numerical results and analyses

A numerical (virtual) EWC (NEWC) with the TAM seated at the table was created, as shown in the two cross-sectional views (side and front) in Fig. 9. CFD simulations were conducted using the NEWC. Boundary conditions were set based on actual experimental conditions as described in the experiments above. The simulations assumed that the wall's temperature was $20\text{ }^{\circ}\text{C}$ and the manikin's body temperature was $37\text{ }^{\circ}\text{C}$. The inlet air velocity was assumed to be 1 m s^{-1} , which matched closely the inlet velocity during the experiments when PIV images were taken.

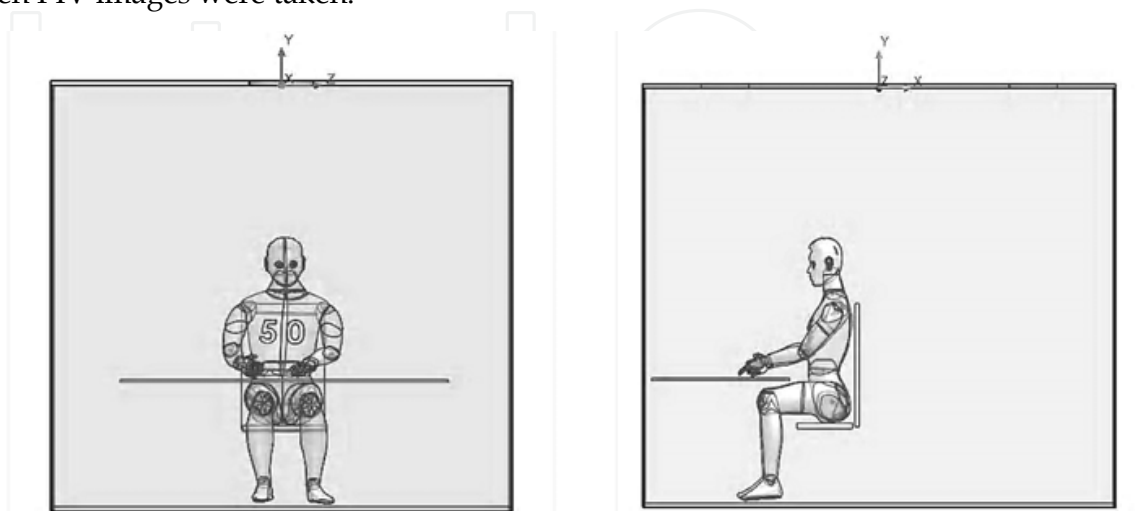


Fig. 9. Front and side views of the NEWC

4.1 Airflow patterns inside NEWC with seated TAM

Fig. 10 shows the air velocity profile (velocity vectors and color-coded velocity range zones) in the vertical middle cross section of the NEWC. Deflection of the air by the table toward the manikin and the opposing wall is clearly seen here as indicated by the vectors. A stagnation area around the inlet axis and accelerated airflow zones along the table surface are also quite visible.

A more detailed velocity field is presented in Fig. 11, with color-coded zones representing the temperature field in the NEWC. To avoid clutter, the velocity field is demonstrated using only 30 trajectories. This figure shows several remarkable stationary eddies that develop near the manikin. The vortex slightly below the head zone and the flow pattern above the table surface were also captured in the PIV experiments. An enlarged section of Fig. 11 is shown in Fig. 12 to elucidate the detailed structure of the flow near the manikin's body.

In the flow near the manikin, body heat contributes to convective airflow along the body, resulting in airflow in the upward direction. If this airflow is contaminated by particles, as from the contaminated foil under study, the flow pattern will certainly result in contamination of the torso. (In fact, Fig. 1 shows that the manikin's torso has become covered with the dust originating from the contaminated foil.) In addition, the stationary eddies that form in front of and behind the head may result in enhanced exposure to the contaminant. Turning the head away from the table may not be helpful in terms of avoiding exposure. Other eddies, such as the ones near the wall and under the table in Fig. 11, may require a longer time to clear the contaminating material from the air in the room.

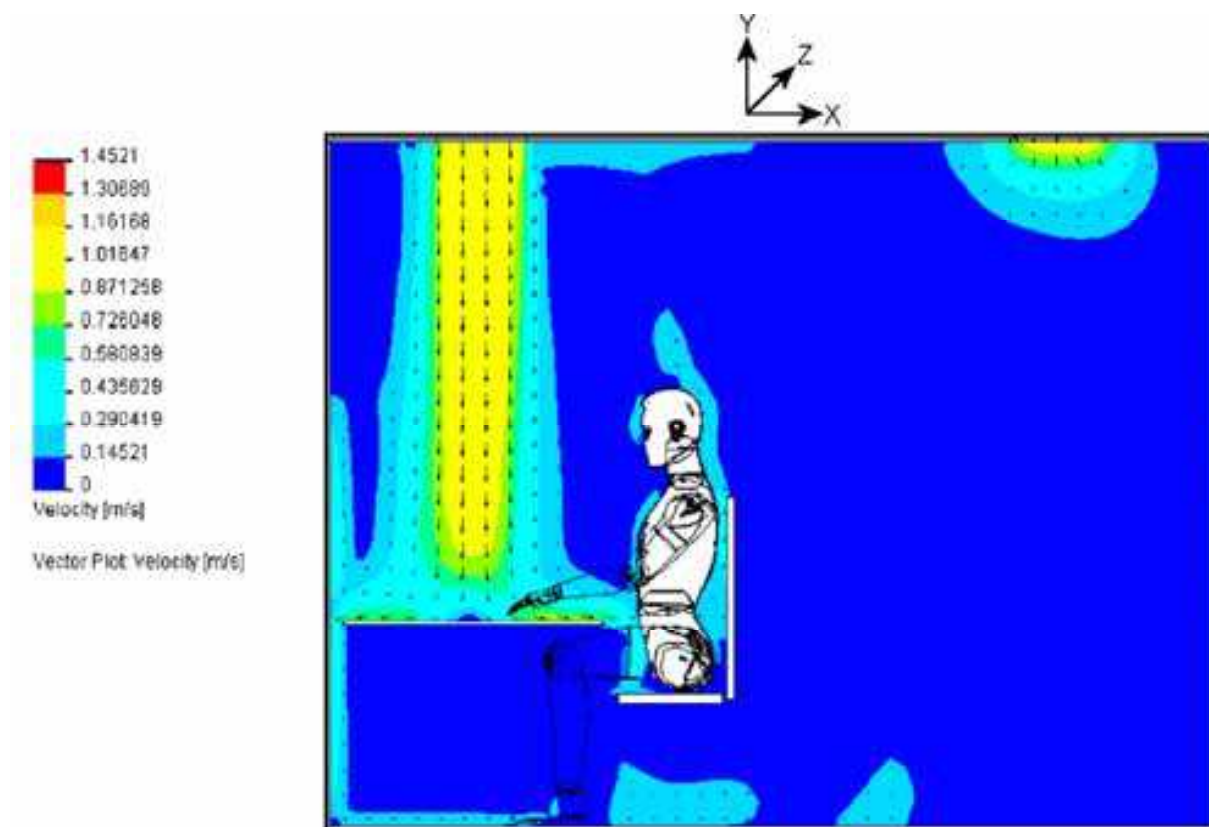


Fig. 10. Air velocity profile in vertical middle cross section of NEWC

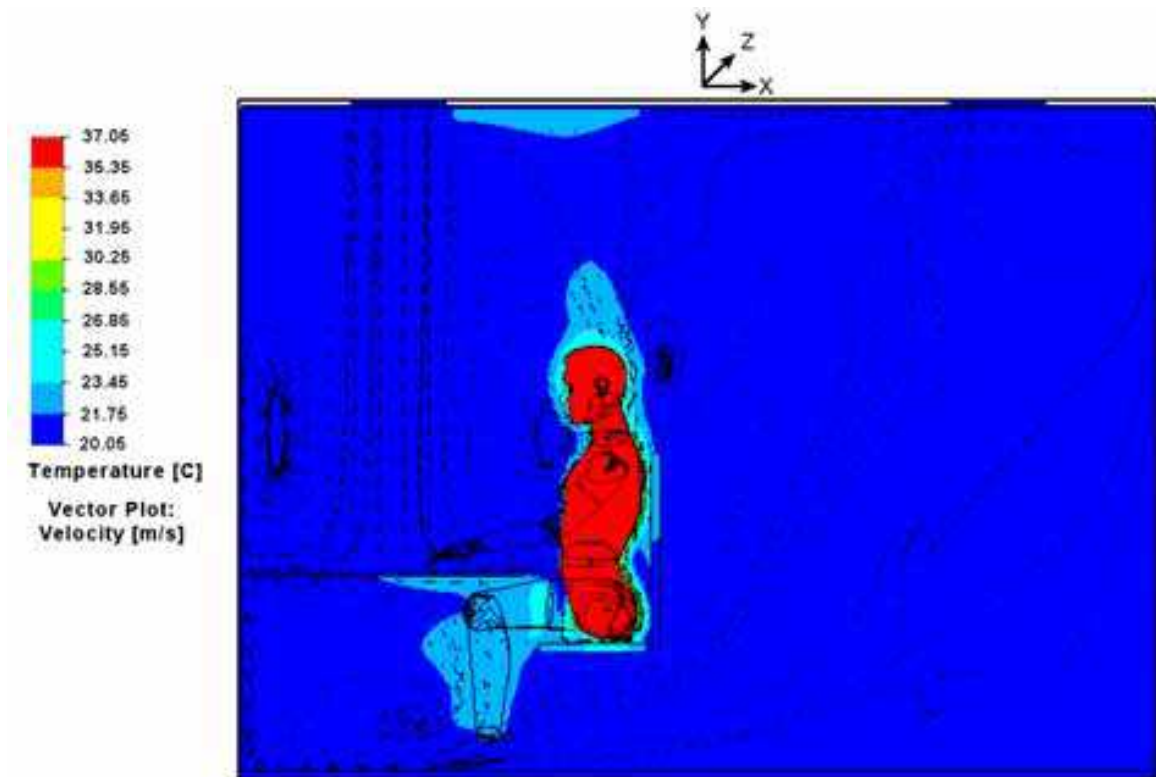


Fig. 11. 2-D air velocity field, represented by 30 trajectories, in vertical middle cross section of NEWC

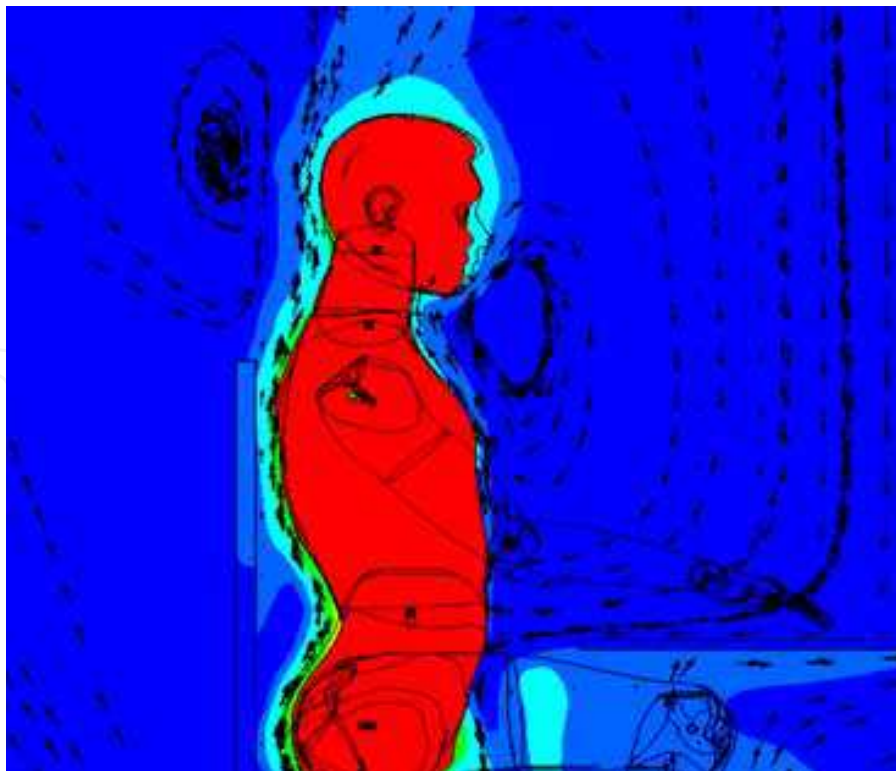


Fig. 12. 2-D flow patterns near manikin's body. Picture is flipped horizontally relative to previous one in order to match the PIV views shown in Fig. 7 and 8.

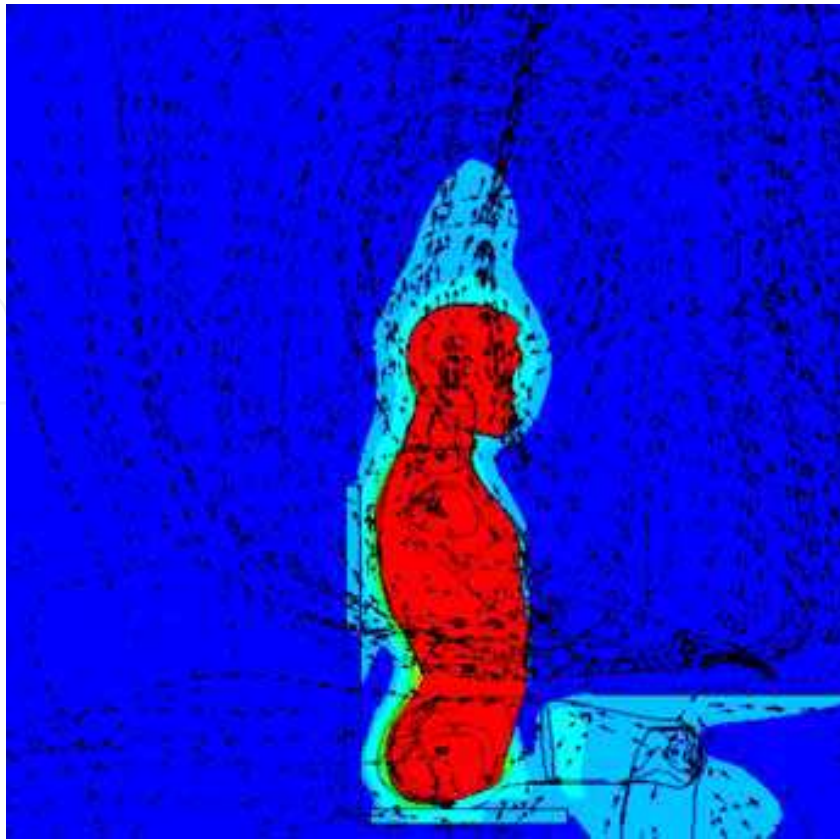


Fig. 13. 3-D flow trajectories inside the NEWC.

In Fig. 13, 3-D flow trajectories from the entire chamber volume are shown as projected onto the central plane. From this figure, one can surmise that the upper torso is essentially engulfed in a complex recirculating vortex. If this air was contaminated, the flow pattern suggests entrapment of the torso in the contaminated personal cloud.

5. Conclusion

The potential exposure of a person to biocontaminants residing on the surface of a letter was examined through experimental and computational evaluation of particle motion and fluid flow between a flat surface and the breathing zone. The scenario examined used an airflow pathway where air is released and withdrawn from ceiling vents on either side of a manikin sitting at a desk in a simulated office enclosure and a black anodized aluminum sheet sprinkled with fine test dust simulating the contaminated letter. Particle imaging velocimetry (PIV) showed that dust from the contaminated sheet could readily reach the torso and the breathing zone of a person sitting next to the letter. Further, extensive contamination of the table and person's body below the table is also likely. Numerical simulations suggest that several recirculating eddies may form in the proximity of the person's head. Such eddies may entrap contaminant particles and thus prolong air contamination and enhance exposure.

The experimental data analyses and numerical modeling described above demonstrate that dust particles originally coating the contaminated letter are dislodged from the letter when it is inadvertently positioned under a ceiling vent. Boundary airflow in the vicinity of the letter causes particle entrainment into the air. Subsequent airflow toward the person's chest

and further vertical airflow is induced by body heat and is sufficient to deliver particles from the contaminated letter to the breathing zone in a couple of seconds. The presence of a recirculating vortex behind the manikin's head suggests that the air behind the manikin rapidly becomes contaminated as well. The flow patterns obtained in numerical simulations suggest that the entire torso will become engulfed in a complex recirculating cloud of particles that leads to its overall contamination.

Based on the experimental and numerical analyses conducted above, it is clear that contaminated dust residing on the surface of a letter would very likely be entrained and transported to the breathing zone of a subject. Further, due to the complex fluid motion generated by the HVAC system, this material is likely to be widely dispersed throughout the office.

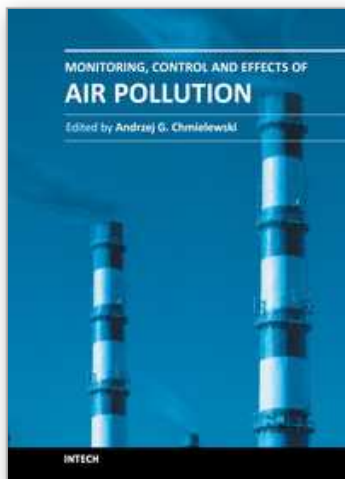
6. Disclaimer

The U.S. Environmental Protection Agency through its Office of Research and Development funded and managed the research described here under Contract EP-D-05-065 with Alion Science and Technology. The views expressed in this paper are those of the authors and do not necessarily reflect the views or policies of the U.S. Environmental Protection Agency. Mention of trade names or commercial products does not constitute endorsement or recommendation for use.

7. References

- Agranovski, E., Pyankov, V. & Altman, S. (2005). Bioaerosol Contamination of Ambient Air as the Result of Opening Envelopes Containing Microbial Materials. *Aerosol Science and Technology*, Vol. 39, No. 11, pp. 1048 – 1055.
- de Armond, P. (2002). The anthrax letters. *Albion Monitor*, <http://www.monitor.net/monitor/0208a/anthrax.html>.
- Block, S., (2001). The growing threat of biological weapons. *American Scientist*, Vol. 89, pp. 28-37.
- Ferziger, H. (1990). Approaches to turbulent flow computation: applications to flow over obstacles. *J Wind Eng Indus Aerodyn*, Vol. 35, pp. 1-19.
- Darrell, W., Pepper, & Xiuling, W., (2007). A meshless model for rapid prediction of indoor contaminant dispersion ICCES, Vol. 13, No. 1, pp.15-21.
- Dull, P., Wilson, K., Kournikakis, B., Whitney, E., Boulet, C., & Ho, J., (2002), Bacillus anthracis aerosolization associated with a contaminated mail-sorting machine. *Emerging Infectious Diseases*, Vol. 8, pp. 1044-1047.
- Duncan, S., Kournikakis, B., & Ho, J. (2009). Pulmonary deposition of aerosolized Bacillus atropheus (BG) in an awake, unrestrained swine model due to exposure from a simulated anthrax letter incident. *Inhalation Toxicology*, Vol. 21, No. 2, pp. 141-152.
- Ho, J. & Fisher, G. (1993). Detection of BW agents: flow cytometry measurement of *Bacillus subtilis* (BG) spore fluorescence. Defense Research Establishment Suffield Technical Memorandum, DRES SM-1421.
- Ho, J. & Duncan, S., (2005). Estimating aerosol hazards from an anthrax letter. *Journal of Aerosol Science*, Vol. 36, pp. 701-719.
- Lien, F., Ji, H., Yee, E., & Kournikakis, B., (2010). Prediction of aerosol hazards arising from the opening of an anthrax-tainted letter in an open office environment using

- computational fluid dynamics. *Journal of Engineering Science and Technology*. Vol. 5, No. 3, pp. 302 - 331.
- Lu, W., Howarth, T, & Jeary, P. (1997). Prediction of airflow and temperature field in a room with convective heat source. *Build Environ*, Vol. 32, No. 6, pp. 541-550.
- Kournikakis, B., Armour, J., Boulet, C.A., Spence, M. & Parsons, B. (2001). Risk assessment of anthrax letters. *Defense Research Establishment Suffield Technical Report*, DRES TR 2001-048.
- Kournikakis, B., Walker, M., Ho, J., & Duncan, S. (2009). Statistical analysis of bacterial spore aerosols created by opening a spore containing "Anthrax Letter" in an office. *Journal of Aerosol Science*, Vol. 40, No. 6, pp. 514-522.
- Kournikakis, B., Ho, J., & Duncan, S. (2010). Anthrax letters: personal exposure, building contamination and effectiveness of immediate mitigation measures. *Journal of Occupational and Environmental Hygiene*, Vol. 7, No. 2, pp. 71-79.
- Mangili A. & Gendreau, A. (2005). Transmission of infectious diseases during commercial air travel. *Lancet*, Vol. 365, pp. 989-994.
- Nardell, A., McInnis, B., Thomas, B. & Weidhaas S. (1986). Exogenous reinfection with tuberculosis in a shelter for the homeless. *New Engl JMed*, No. 315, pp. 1570-1571.
- NATO Programme for Security through Science. (2005). Risk Assessment and Risk Communication Strategies in Bioterrorism Preparedness. In Green MS, Zenilman, J., Cohen, D., Wiser, I. & Balicer, D., editors. NATO Security through Science Series - A: Chemistry and Biology. The Netherlands: Springer. ISBN 978-1-4020-5807-3 (PB), ISBN 978-1-4020-5806-6 (HB).
- Nazaroff, W. (2004). Indoor particle dynamics. *Indoor Air*, Vol. 14, pp. 175-183.
- Patankar, S. (1980). *Numerical heat transfer and fluid flow*. Hemisphere Publishing Corporation.
- Posner, D., Buchanan, R. & Dunn-Rankin D. (2003). Measurement and prediction of indoor air flow in a model room. *Energ Build*, Vol. 35, No. 5, pp. 515-526.
- Price, P., Sohn, M., Lacomme, K. & McWilliams, J. (2009). Framework for evaluating anthrax risk in buildings. *Environmental Science and Technology*, Vol. 43, No. 6, pp. 1783-1787.
- Reshetin, V., & Regens, J., (2003). Simulation modeling of anthrax spore dispersion in a bioterrorism incident. *Risk Analysis*, Vol. 23, pp. 1135-1145.
- Reshetin, V., & Regens, D. (2004). Evaluation of malignant anthrax spore dispersion in high-rise buildings. *Journal of Engineering Physics and Thermophysics*, Vol. 77, No. 6, pp.1155-1166.
- Rhie, C. & Chow, W., (1983). A numerical study of the turbulent flow past an isolated airfoil with trailing edge separation. *AIAA Journal*, Vol. 21, No. 11, pp. 1525-1532.
- Richmond-Bryant, J., Eisner, A., Brixey, L., & Wiener, R. (2006). Short-term dispersion of indoor aerosols: can it be assumed the room is well mixed? *Building and Environment*, Vol. 41, No. 2, pp. 156-162.
- Rim, D. & Novoselac, A. (2009). Transport of particulate and gaseous pollutants in the vicinity of human body. *Build Environ*, Vol. 44, pp. 1840-1849.
- Vlahostergios, Z., Yakinthos, K. & Goulas, A. (2009). Separation-induced boundary layer transition: modeling with a non-linear eddy-viscosity model coupled with the laminar kinetic energy equation. *Int JHeat Fluid Fl*, Vol. 30, No. 4, pp. 617-636.
- Wallace, L. (1996). Indoor particles: a review. *JAir Waste Manage Assoc*, Vol. 46, pp. 98-126.



Monitoring, Control and Effects of Air Pollution

Edited by Prof. Andrzej G. Chmielewski

ISBN 978-953-307-526-6

Hard cover, 254 pages

Publisher InTech

Published online 23, August, 2011

Published in print edition August, 2011

The book addresses the subjects related to the selected aspects of pollutants emission, monitoring and their effects. The most of recent publications concentrated on the review of the pollutants emissions from industry, especially power sector. In this one emissions from opencast mining and transport are addressed as well. Beside of SO_x and NO_x emissions, small particles and other pollutants (e.g. VOC, ammonia) have adverse effect on environment and human being. The natural emissions (e.g. from volcanoes) has contribution to the pollutants concentration and atmospheric chemistry governs speciation of pollutants, as in the case of secondary acidification. The methods of ambient air pollution monitoring based on modern instrumentation allow the verification of dispersion models and balancing of mass emissions. The comfort of everyday human's activity is influenced by indoor and public transport vehicles interior air contamination, which is effected even by the professional appliances operation. The outdoor pollution leads to cultural heritage objects deterioration, the mechanism are studied and the methods of rehabilitation developed. However to prevent emissions the new technologies are being developed, the new class of these technologies are plasma processes, which are briefly reviewed at the final part of the book.

How to reference

In order to correctly reference this scholarly work, feel free to copy and paste the following:

Alfred D. Eisner, Russell W. Wiener and Jacky Rosati (2011). In-Office Dispersion and Exposure to Contaminants Originating from an Unfolded Letter, Monitoring, Control and Effects of Air Pollution, Prof. Andrzej G. Chmielewski (Ed.), ISBN: 978-953-307-526-6, InTech, Available from:
<http://www.intechopen.com/books/monitoring-control-and-effects-of-air-pollution/in-office-dispersion-and-exposure-to-contaminants-originating-from-an-unfolded-letter>

INTECH
open science | open minds

InTech Europe

University Campus STeP Ri
Slavka Krautzeka 83/A
51000 Rijeka, Croatia
Phone: +385 (51) 770 447
Fax: +385 (51) 686 166
www.intechopen.com

InTech China

Unit 405, Office Block, Hotel Equatorial Shanghai
No.65, Yan An Road (West), Shanghai, 200040, China
中国上海市延安西路65号上海国际贵都大饭店办公楼405单元
Phone: +86-21-62489820
Fax: +86-21-62489821

© 2011 The Author(s). Licensee IntechOpen. This chapter is distributed under the terms of the [Creative Commons Attribution-NonCommercial-ShareAlike-3.0 License](#), which permits use, distribution and reproduction for non-commercial purposes, provided the original is properly cited and derivative works building on this content are distributed under the same license.

IntechOpen

IntechOpen